

AFRL-SN-WP-TP-2002-101

**COMPARISON OF SURFACE
PASSIVATION FILMS FOR REDUCTION
OF CURRENT COLLAPSE IN AlGaIn/GaN
HIGH ELECTRON MOBILITY
TRANSISTORS (HEMTs)**



**R. Fitch, J. Gillespie, T. Jenkins, J. Sewell, D. Via, and
A. Crespo (AFRL/SNDD)**

B. Luo, R. Mehandru, J. Kim, and F. Ren (U of F Chem. Eng.)

**B. P. Gila, A. H. Onstine, C. R. Abernathy, and S. J. Pearton (U of F Matls. Sci.
Eng.)**

Y. Irokawa (Toyota)

MARCH 2002

Approved for public release; distribution unlimited.

**This material is declared a work of the U.S. Government and is not subject to
copyright protection in the United States.**

**SENSORS DIRECTORATE
AIR FORCE RESEARCH LABORATORY
AIR FORCE MATERIEL COMMAND
WRIGHT-PATTERSON AIR FORCE BASE, OH 45433-7318**


20020610 102

NOTICE

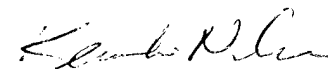
USING GOVERNMENT DRAWINGS, SPECIFICATIONS, OR OTHER DATA INCLUDED IN THIS DOCUMENT FOR ANY PURPOSE OTHER THAN GOVERNMENT PROCUREMENT DOES NOT IN ANY WAY OBLIGATE THE US GOVERNMENT. THE FACT THAT THE GOVERNMENT FORMULATED OR SUPPLIED THE DRAWINGS, SPECIFICATIONS, OR OTHER DATA DOES NOT LICENSE THE HOLDER OR ANY OTHER PERSON OR CORPORATION; OR CONVEY ANY RIGHTS OR PERMISSION TO MANUFACTURE, USE, OR SELL ANY PATENTED INVENTION THAT MAY RELATE TO THEM.

THIS REPORT IS RELEASABLE TO THE NATIONAL TECHNICAL INFORMATION SERVICE (NTIS). AT NTIS, IT WILL BE AVAILABLE TO THE GENERAL PUBLIC, INCLUDING FOREIGN NATIONS.

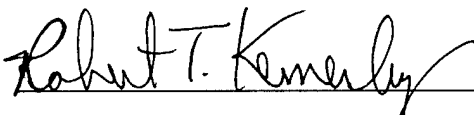
THIS TECHNICAL REPORT HAS BEEN REVIEWED AND IS APPROVED FOR PUBLICATION.



GLEN D. VIA, Project Engineer
Electron Devices Branch
Aerospace Components Division



KENICHI NAKANO, Chief
Electron Devices Branch
Aerospace Components Division



ROBERT T. KEMERLEY, Chief
Aerospace Components Division
Sensors Directorate

Do not return copies of this report unless contractual obligations or notice on a specific document require its return.

REPORT DOCUMENTATION PAGE				Form Approved OMB No. 074-0188	
Public reporting burden for this collection of information is estimated to average 1 hour per response, including the time for reviewing instructions, searching existing data sources, gathering and maintaining the data needed, and completing and reviewing this collection of information. Send comments regarding this burden estimate or any other aspect of this collection of information, including suggestions for reducing this burden to Washington Headquarters Services, Directorate for Information Operations and Reports, 1215 Jefferson Davis Highway, Suite 1204, Arlington, VA 22202-4302, and to the Office of Management and Budget, Paperwork Reduction Project (0704-0188), Washington, DC 20503					
1. AGENCY USE ONLY (Leave blank)		2. REPORT DATE March 2002		3. REPORT TYPE AND DATES COVERED Preprint, 01/07/2002 – 03/08/2002	
4. TITLE AND SUBTITLE Comparison of Surface Passivation Films for Reduction of Current Collapse in AlGaIn/GaN High Electron Mobility Transistors (HEMTs)				5. FUNDING NUMBERS C: In-House PE: N/A PR: N/A TA: N/A WU: N/A	
6. AUTHOR(S) R. Fitch, J. Gillespie, T. Jenkins, J. Sewell, D. Via, A. Crespo (AFRL/SNDD) B. Luo, R. Mehandru, J. Kim, and F. Ren (U o F Chem. Eng.) B. P. Gila, A. H. Onstine, C. R. Abernathy, and S. J. Pearton (U o F Matls. Sci. Eng.) Y. Irokawa (Toyota)					
7. PERFORMING ORGANIZATION NAME(S) AND ADDRESS(ES) Electron Devices Branch (AFRL/SNDD) Aerospace Components and Subsystems Technology Division Sensors Directorate Air Force Research Laboratory Air Force Materiel Command WPAFB, OH 45433-7318				8. PERFORMING ORGANIZATION REPORT NUMBER AFRL-SN-WP-TP-2002-101	
9. SPONSORING / MONITORING AGENCY NAME(S) AND ADDRESS(ES) SENSORS DIRECTORATE AIR FORCE RESEARCH LABORATORY AIR FORCE MATERIEL COMMAND WRIGHT-PATTERSON AIR FORCE BASE, OH 45433-7318 POC: Glen D. Via, AFRL/SNDD, (937) 255-1874 x3457				10. SPONSORING / MONITORING AGENCY REPORT NUMBER AFRL-SN-WP-TP-2002-101	
11. SUPPLEMENTARY NOTES This material is declared a work of the U.S. Government and is not subject to copyright protection in the United States. Article submitted for publication to <i>Journal of Applied Physics</i> , pending acceptance. Vertical axis text on figure labels overlaps.					
12a. DISTRIBUTION / AVAILABILITY STATEMENT Approved for public release; distribution unlimited.					12b. DISTRIBUTION CODE
13. ABSTRACT (Maximum 200 Words) Three different passivation layers (SiNx, MgO, and Sc2O3) were examined for their effectiveness in mitigating surface-state-induced current collapse in AlGaIn/GaN high electron mobility transistors (HEMTs). The plasma-enhanced chemical vapor deposited SiNx produced ~70 to 75 percent recovery of the drain-source current, independent of whether SiH4/NH3 or SiD4/ND3 plasma chemistries were employed. Both the Sc2O3 and MgO produced essentially complete recover of the current in GaN-cap HEMP structures and ~80 to 90 percent recovery in AlGaIn-cap structures. The Sc2O3 had superior long-term stability, with no change in HEMT behavior over 5 months of aging.					
14. SUBJECT TERMS Gallium Nitride, Wide Bandgap Devices, Passivation				15. NUMBER OF PAGES 28	
				16. PRICE CODE	
17. SECURITY CLASSIFICATION OF REPORT Unclassified	18. SECURITY CLASSIFICATION OF THIS PAGE Unclassified	19. SECURITY CLASSIFICATION OF ABSTRACT Unclassified		20. LIMITATION OF ABSTRACT SAR	

NSN 7540-01-280-5500

Standard Form 298 (Rev. 2-89)
Prescribed by ANSI Std. Z39-18
298-102

INTRODUCTION

AlGaIn/GaN high electron mobility transistors (HEMTs) show great promise for applications in which high speed and high temperature operation are required, such as high frequency wireless base stations and broad-band links, commercial and military radar and satellite communications [1-30]. These devices appear capable of producing very high power densities ($>12\text{W}\cdot\text{mm}^{-1}$), along with low noise figures (0.6dB at 10GHz) and high breakdown voltage. A number of recent reviews have appeared on this topic[31-35]. The use of metal-oxide-semiconductor (MOS) or metal-insulator-semiconductor (MIS) gates for HEMTs produces a number of advantages over the more conventional Schottky metal gates, including lower leakage current and greater voltage swing [3, 22, 26, 28-30]. Amongst the materials employed for gate oxide/insulators are SiO_2 [3, 25-30, 42, 43], $\text{Gd}(\text{Ga}_2\text{O}_3)$ [25, 26, 30, 40], AlN [41], SiN_x [16, 36-39], MgO [27, 44] and Sc_2O_3 [44]. These materials can also be employed as surface passivation layers on HEMTs. One problem commonly observed in these devices is the so-called "current collapse" in which the application of a high drain-source voltage leads to a decrease of the drain current and increase in the knee voltage [5, 7, 14-20, 23]. This phenomenon can also be observed by a current dispersion between dc and pulsed test conditions or a degraded rf output power. The cause is the presence of surface states on the cap layer or trapping centers in the resistive buffer underlying the active channel. The carriers in the 2-dimensional electron gas can be lost either to the surface or buffer traps [5, 7, 45-48]. The former may be mitigated to a greater or lesser extent by use of appropriate surface passivation, most often SiN_x deposited by plasma-enhanced chemical vapor deposition (PECVD), while the latter is a function of the epitaxial growth conditions. In the situation in which surface states dominate the current collapse, the use of SiN_x passivation typically restores 70-80% of the "lost" current.

We have recently found promising results for two alternative candidates for HEMT passivation, namely Sc_2O_3 and MgO [49, 50]. A comparison of the properties of these oxides with those of the other commonly used passivation materials on GaN is shown in Table I. They have smaller lattice mismatch to GaN and larger bandgap than Gd_2O_3 . In addition, they do not contain hydrogen and may have advantages over SiN_x in that respect because atomic hydrogen diffuses rapidly and could enter the GaN or gate metal over extended periods of device operation.

In this paper we report on a comparison of SiN_x , MgO and Sc_2O_3 passivation layers on AlGaIn/GaN HEMTs with different layer structures (GaN vs AlGaIn cap layer) and show the long-term (5 month) stability of the MgO and Sc_2O_3 passivation. We find essentially complete mitigation of the drain current collapse in GaN-capped HEMTs passivated with MgO or Sc_2O_3 , compared to 70-75% recovery with SiN_x . For AlGaIn-capped HEMTs, the MgO and Sc_2O_3 is effective in restoring ~80-90% of the drain current.

EXPERIMENTAL

Two different HEMT structures were used in these experiments. The first employed a GaN undoped cap layer on top of an undoped $\text{Al}_{0.2}\text{Ga}_{0.8}\text{N}$ layer. Both Al_2O_3 and SiC

substrates were used. The doping in this structure is basically due to piezo-induced carriers. The second type of HEMT employed an undoped $\text{Al}_{0.3}\text{Ga}_{0.7}\text{N}$ cap layer on top of a doped $\text{Al}_{0.3}\text{Ga}_{0.7}\text{N}$ donor layer. The doping in this structure is due to the intentional Si-doping of the donor layer. The ohmic (Ti/Al/Pt/Au) and gate (Ni/Au) contacts were deposited by e-beam evaporation and patterned by lift-off. Schematics of the completed device structures are shown in Figure 1.

The 100Å thick MgO , Sc_2O_3 or SiN_x layers were deposited on completed devices (0.25-1.2µm gate length, 100µm gate width) using either Molecular Beam Epitaxy (MBE) for the oxides or PECVD for the SiN_x , with deposition temperatures of 100°C in the oxide case and 250°C for the SiN_x case. Details of the oxide deposition have been given previously [49-50]. The SiN_x films were deposited with either $\text{SiH}_4 + \text{NH}_3$ or $\text{SiD}_4 + \text{ND}_3$ to examine the effect of deuterated precursors.

The HEMT dc parameters were measured in dc and pulsed mode at 25°C, using a parameter analyzer for the dc measurements and pulse generator, dc power supply and oscilloscope for the pulsed measurements. For the gate lag measurements, the gate voltage V_G was pulsed from -5V to 0V at different frequencies with a 10% duty cycle.

RESULTS AND DISCUSSION

(a) Unpassivated Devices

Figure 2 (top) shows typical gate lag data for $0.5 \times 100\mu\text{m}^2$ GaN-cap HEMT grown on sapphire substrates. The decrease in drain-source current becomes more pronounced at high measurement frequencies. The degradation in current was less significant when these same structures were grown on SiC substrates, as shown in Figure 2 (bottom). The defect density will be lower in the latter case due to the closer lattice match between GaN and SiC and this appears to affect the resultant surface state density. This suggests that at least some of the surface traps are related to dislocations threading to the surface.

The effects of both substrate type and HEMT gate length on the change in drain-source current are shown in Figure 3. The shorter the gate length, the more pronounced the degradation in current because of larger surface area and higher electric field in the channel between source (S) and drain (D). The S-D distance was fixed in all cases.

(b) SiN_x Passivation

Figure 4 (top) shows the $I_{\text{DS}}-V_{\text{DS}}$ characteristics before and after SiN_x passivation using either hydrogenated or deuterated precursors. The inset shows the complete set of curves for the as-fabricated HEMT and the main figure shows only the uppermost curves for clarity. The I_{DS} increases after passivation with either type of SiN_x , which indicates that the surface state density is decreased [15]. Similarly, the transconductance (g_m) increases after SiN_x deposition, which also suggests a decrease in surface trap density (Figure 4, bottom) [15].

The gate lag data is shown in Figure 5 (top) for the HEMTs before and after SiN_x passivation. Note that both the hydrogenated and deuterated precursor dielectric

produces a recovery of 70-75% in the drain-source current. This range represents results obtained from five different devices with each type of dielectric. The unity current gain frequency (f_T) and maximum frequency of oscillation (f_{MAX}) data before and after passivation are shown at the bottom of Figure 5. Note that there is actually a slight increase in both parameters, in contrast to previous reports [15]. There were no systematic differences between the results for hydrogenated and deuterated precursor SiN_x , even though the latter typically produce slightly denser films when deposited under the same PECVD conditions.

There was also an increase in forward and reverse gate currents after passivation with SiN_x , as shown in the I-V characteristics in Figure 6. These results are also consistent with a decrease in surface depletion and decrease in surface trap density and indicate that there is no major degradation to the dc performance of the HEMTs upon addition of the SiN_x layer. We believe the increase in gate leakage is not from the passivation itself, but may originate from degradation of the gate metalization during the oxide desorption step at 350°C.

(c) MgO and Sc_2O_3 Passivation of GaN-cap HEMTs

Figure 7 shows the gate lag data for GaN-cap $0.5 \times 100 \mu\text{m}^2$ HEMTs. In the case at top, V_G was pulsed from -5 to 0V at 0.1MHz with a 10% duty cycle and this pulsed data is compared to that from dc measurements. The bottom of Figure 7 shows the normalized I_{DS} for gate voltage switched from -5V with V_{DS} held constant at 3V to avoid any self-heating effects. This data establishes the base-line for measuring the effectiveness of the MgO and Sc_2O_3 passivation. As reported previously [45], these HEMTs showed an increase in drain-source current of ~20% after deposition of either type of oxide. In addition, the forward and reverse gate currents were slightly increased (Figure 8 shows an example for an MgO -passivated HEMT). These results are similar to those for SiN_x deposition. Once again, the increased reverse current may be due to gate metal degradation.

Figure 9 shows gate lag measurement for MgO -passivated HEMTs immediately after MgO deposition and after 5 months aging without bias on the devices under room conditions (temperature and humidity). The I_{DS} increases ~20% upon passivation, as mentioned earlier and there is almost complete mitigation of the degradation in I_{DS} immediately after MgO deposition. However after 5 months aging, there is a clear difference between the dc and pulsed data, indicating that the MgO passivation has lost some of its effectiveness. We are currently investigating possible mechanisms such as oxidation of the GaN surface through pinholes in the MgO , or reaction between the MgO and GaN.

Similar data is shown in Figure 10 for Sc_2O_3 -passivated HEMTs. In this data the I_{DS} also increases upon deposition of the oxide and there is also essentially complete mitigation of the degradation in drain-source current. However, the major difference is that there is no significant change in these characteristics after 5 months aging. This indicates that Sc_2O_3 provides more stable passivation than MgO . We have noticed in separate experiments

that the MgO/GaN interface deteriorates over time if left uncapped, i.e. we see increases in interface state trap density in MOS diodes on which the metal is deposited a long period after the MgO was deposited on the GaN. However, if the MgO is immediately covered by the gate metal these changes are not observed. In a real manufacturing process, the MgO-passivated HEMTs would be covered with a dielectric such as SiN_x to provide mechanical protection and therefore MgO should not be disqualified as a candidate to provide effective passivation of GaN/AlGaN HEMTs. Obviously, further work is needed to establish the reliability of Sc_2O_3 and MgO passivation on these devices, but the preliminary data with Sc_2O_3 looks very promising.

(d) MgO and Sc_2O_3 passivation of AlGaN-cap HEMTs

Figure 11 shows the gate lag data for the HEMT structures of Figure 1 (bottom), i.e. the structures with $\text{Al}_{0.3}\text{Ga}_{0.7}\text{N}$ as the top layer. As with the GaN-cap devices, there is a very significant degradation of drain-source current under pulsed conditions where the surface traps cannot completely empty.

The effectiveness of the MgO and Sc_2O_3 passivation was more variable on the AlGaN-cap devices than for the GaN-capped HEMTs described in the previous section. Figure 12 shows typical gate-lag data from a Sc_2O_3 passivated AlGaN-cap HEMT. We found that the Sc_2O_3 deposition was typically able to restore 80-90% of the drain current loss relative to dc measurement conditions. Some devices showed essentially complete restoration of the current, but the 80-90% range was more typical. Similar results were obtained for MgO passivation, as shown in Figure 13. Once again, some individual HEMTs showed essentially full restoration of I_{DS} upon MgO deposition, but a more typical result was that shown in Figure 13, with 80-90% effectiveness. We believe that our in-situ cleaning procedure prior to deposition of these oxides in the MBE chamber is not able to completely remove the native oxide from the AlGaN surface. This limits the effectiveness of the resulting passivation and accounts for the more variable results we observe for the AlGaN-cap devices.

SUMMARY AND CONCLUSIONS

MgO and Sc_2O_3 thin films deposited by MBE appear very promising as surface passivation layers on AlGaN/GaN HEMTs. In our structures with a GaN-cap layer they provide more effective mitigation of drain current collapse than the conventional PECVD SiN_x films. The Sc_2O_3 provides stable passivation characteristics over a period of at least 5 months, while the MgO was found to lose some of its effectiveness under the same conditions. The passivation with both oxides is more variable on AlGaN-cap structures, which we believe is due to the greater difficulties in removing the native oxide from the AlGaN surface prior to deposition of the passivation films. With respect to SiN_x passivation, we found no obvious advantage to the use of deuterated precursors for the deposition. Finally, it should be noted that both MgO and Sc_2O_3 can also be used as gate dielectrics on GaN to provide MOS diodes and transistors and thus an MBE system equipped for their deposition can provide both the gate oxide and the device passivation in a manufacturing environment.

ACKNOWLEDGEMENTS

The work at UF was partially supported by ONR (H. B. Dietrich, N00014-1-02-04) and NSF (DMR010438 and CTS 9901173).

REFERENCES

1. N. X. Nguyen, M. Micovic, W.-S. Wong, P. Hashimoto, L.-M. McCray, P. Janke, C. Nguyen, *Electron. Lett.* **36**, 468(2000).
2. Y. -F. Wu, B. P. Keller, S. Keller, D. Kapolnek, P. Kozodoy, S. P. DenBaars and U. K. Mishra, *Solid-State Electron.*, **41**, 1569(1997).
3. M. A. Khan, X. Hu, G. Simin, A. Lunev, J. Yang, R. Gaska, and M.S. Shur, *IEEE Electron. Dev. Lett.* **21**, 63(2000).
4. K. K. Chu, J. A. Smart, J. R. Shealy and L. F. Eastman, Proc. State-of-The-Art Program on Compound Semiconductors (SOTAPOCS XX/X, Electrochem. Soc., Pennington, NJ 1998), M.3-12.
5. B. M. Green, K. K. Chu, E. M. Chumbes, J. A. Smart, J. R. Shealy, and L. F. Eastman, *IEEE Electron. Dev. Lett.*, **21**, 268(2000).
6. S. C. Binari, W. Kruppa, H. B. Dietrich, G. Kelner, A. E. Wickenden and J. A. Freitas Jr, *Solid-State Electron.*, **41**, 1549(1997).
7. L. F. Eastman, V. Tilak, J. Smart, B. M. Green, E. M. Chumbes, R. Dimitrov, H. Kim; O. S. Ambacher, N. Weimann, T. Prunty, M. Murphy, W. J. Schaff, and J. R. Shealy, *IEEE Trans. Electron Dev.*, **48**, 479(2001).
8. Y. -F. Wu, B. P. Keller, S. Keller, D. Kapolnek, P. Kozodoy, S. P. DenBaars and U. K. Mishra, *Solid-State Electron.*, **41**, 1569(1997).
9. J. W. Johnson, A.G. Baca, R. D. Briggs, R. J. Shul, C. Monier, F. Ren, S. J. Pearton, A. M. Dabiran, A. M. Wowchack, C. J. Polley and P. P. Chow, *Solid-State Electron.*, **45**, 1979(2001).
10. W. Lu, J. Yang, M. A. Khan and I. Adesida, *IEEE Trans. Electron Dev.*, **ED48**, 581(2001).
11. S. J. Pearton, J. C. Zolper, R. J. Shul and F. Ren, *J. Appl. Phys.*, **86**, 1(1999).
12. M. Asif Khan, Q. Chen, Michael S. Shur, B. T. Dermott, J. A. Higgins, J. Burm, W. J. Schaff and L. F. Eastman, *Solid-State Electron.*, **41**, 1555(1997).
13. G. Simin, X. Hu, N. Ilinskaya, A. Kumar, A. Koudymov, J. Zhang, M. Asif Khan, R. Gaska, M. S. Shur, *Electron. Lett.* **36**, 2043(2000).
14. E. Kohn, I. Daumiller, P. Schmid, N. X. Nguyen, C. N. Nguyen, *Electron. Lett.* **35**, 1022(1999).
15. J.-S. Lee; A. Vescan, A. Wieszt, R. Dietrich, H. Leier, Y.-S. Kwon, *Electron. Lett.* **37**, 130(2001).
16. X. Hu, A. Koudymov, G. Simin, J. Yang, M. Asif Khan, A. Tarakji, M. S. Shur, and R. Gaska, *Appl. Phys. Lett.* **79**, 2832(2001).
17. N. X. Nguyen, C. Nguyen and D. E. Grider, *Electron. Lett.* **35**, 1356(1999).
18. I. Daumiller, C. Kirchner, M. Kamp, K. J. Ebeling, and E. Kohn, *IEEE Electron. Dev. Lett.* **20**, 448(1999).
19. A. Tarakji, G. Simin, N. Ilinskaya, X. Hu, A. Kumar, A. Koudymov, J. Yang, M. Asif Khan, M. S. Shur, and R. Gaska, *Appl. Phys. Lett.* **78**, 2169(2001).

20. E. M. Chumbes, J. A. Smart, T. Prunty and J. M. Shealy, *IEEE Trans. Electron Dev.*, **48**, 416(2001).
21. B. Luo, J. W. Johnson, F. Ren, K. K. Allums, C. R. Abernathy, S. J. Pearton, R. Dwivedi, T. N. Fogarty, R. Wilkins, A. M. Dabiran, A. M. Wowchack, C. J. Polley, P. P. Chow and A. G. Baca, *Appl. Phys. Lett.*, **79**, 2196(2001).
22. S. J. Pearton, F. Ren, A. P. Zhang and K. P. Lee, *Mat. Sci. Eng. Rep. R30*, 55(2000).
23. S. C. Binari, K. Ikossi, J. A. Roussos, W. Kruppa, D. Park; H. B. Dietrich, D. D. Koleske, A. E. Wickenden, and R. L. Henry, *IEEE Trans. Electron Dev.*, **48**, 465(2001).
24. G. Simin, A. Koudymov, A. Tarakji, X. Hu, J. Yang, M. Asif Khan, M. S. Shur, and R. Gaska, *Appl. Phys. Lett.* **79**, 2651(2001).
25. F. Ren, M. Hong, S. N. G. Chu, M. A. Marcus, M. J. Schurman, A. Baca, S. J. Pearton, and C. R. Abernathy, *Appl. Phys. Lett.*, **73**, 3893(1998).
26. J. W. Johnson, B. Luo, F. Ren, B. P. Gila, V. Krishnamoorthy, C. R. Abernathy, S. J. Pearton, J. I. Chyi, T. E. Nee, C. M. Lee, and C. C. Chuo, *Appl. Phys. Lett.*, **77**, 3230(2000).
27. B. P. Gila, J. W. Johnson, K. N. Lee, V. Krishnamoorthy, C. R. Abernathy, F. Ren, and S. J. Pearton, *ECS Proc. Vol.*, **2001-1**, 71(2001).
28. M. Asif Khan, X. Hu, A. Tarakji, G. Simin, J. Yang, R. Gaska, and M. S. Shur, *Appl. Phys. Lett.* **77**, 1339(2001).
29. G. Simin, X. Hu, N. Ilinskaya, J. Zhang, A. Tarakji, A. Kumar, J. Yang, M. Asif Khan, R. Gaska, M. S. Shur, *IEEE Electron. Dev. Lett.* **22**, 53(2001).
30. J. W. Johnson, B. P. Gila, B. Luo, K. P. Lee, C. R. Abernathy, S. J. Pearton, J. I. Chyi, T. E. Nee, C. M. Lee, C. Chou and F. Ren, *J. Electrochem. Soc.* G303(2001).
31. M. S. Shur, *Solid-State Electron.* **42**, 2131(1998).
32. Hadis Morkoç, Aldo Di Carlo and Roberto Cingolani, *Solid-State Electron.* **46**, 157(2002).
33. Y. Ohno, M. Kuzuhara, *IEEE Trans. Electron Dev.* **ED48**, 517(2001).
34. Y.-F. Wu; D. Kapolnek, J. P. Ibbetson, P. Parikh, B. P. Keller, U. K. Mishra, *IEEE Trans. Electron Dev.* **ED48**, 586(2001).
35. H. Morkoc, *Nitride Semiconductors and Devices* (Springer, Berlin, 1999).
36. B. Gaffey, L. J. Guido, X. W. Wang, and T. P. Ma, *IEEE Trans. Electron Dev.* **ED48**, 458(2001).
37. Steven C. Binari, K. Doverspike, G. Kelner, H. B. Dietrich and A. E. Wickenden, *Solid-State Electron.* **41**, 177(1997).
38. S. Arulkumaran, T. Egawa, H. Ishikawa, T. Jimbo, and M. Umeno, *Appl. Phys. Lett.* **73**, 809(1998).
39. I. Irokawa and Y. Nakano, *Solid-State Electron.* (In press).
40. T. S. Lay, M. Hong, J. Kwo, J. P. Mannaerts, W. H. Hung and D. J. Huang, *Solid-State Electron.* **45**, 1679(2001).
41. T. Hashizume, E. Alekseev, D. Pavlidis, K. S. Boutros, and J. Redwing, *J. Appl. Phys.* **88**, 1983(2000).
42. N.-Q. Zhang, S. Keller, G. Parish, S. Heikman, S. P. DenBaars, U. K. Mishra, *IEEE Electron. Dev. Lett.* **21**, 421(2000).
43. R. Therrien, G. Lucovsky and R. F. Davis, *Phys. Stat. Solidi.* **A176**, 793(1999).

44. B. P. Gila, J. Johnson, R. Mehandra, B. Luo, A. H. Onstine, K. K. Allums, V. Krishamoorthy, S. Bates, C. R. Abernathy, F. Ren, and S. J. Pearton, *Phys. Stat. Solidi A* **188**, 239(2001).
45. P. B. Klein, S. C. Binari, K. Ikossi, A. E. Wickenden, D. D. Koleske, and R. L. Henry, *Appl. Phys. Lett.* **79**, 3527(2001).
46. P. B. Klein, J. A. Freitas, Jr., S. C. Binari, and A. E. Wickenden, *Appl. Phys. Lett.* **75**, 4016(1999).
47. P. B. Klein, S. C. Binari, J. A. Freitas, Jr., and A. E. Wickenden, *J. Appl. Phys.* **88**, 2843(2000).
48. P. B. Klein, S. C. Binari, K. Ikossi-Anastasiou, A. E. Wickenden, D. D. Koleske, P. L. Henry, D. S. Katzer, *IEEE Electron. Lett.* **37**, 661(2001).
49. B. Luo, J. W. Johnson, J. Kim, R. M. Mehandru, F. Ren, B. P. Gila, A. H. Onstine, C. R. Abernathy, S. J. Pearton, A. G. Baca, R. D. Briggs, R. J. Shul, C. Monier, and J. Han, *Appl. Phys. Lett.* **80**, 1661(2002).
50. B. Luo, J. W. Johnson, B. P. Gila, A. Onstine, C. R. Abernathy, F. Ren, S. J. Pearton, A. G. Baca, A. M. Dabiran, A. M. Wowchack and P. P. Chow, *Solid-State Electron.* **46**, 467(2002).

Table I: Material properties for GaN and various dielectrics. W = Wurtzite, A = amorphous, B = Bixbyite, N = NaCl.

	GaN [a]	SiO ₂ [b-d]	SiN _x [d]	AlN [e-g]	GGG [h]	Gd ₂ O ₃ [h-j]	Sc ₂ O ₃ [k]	MgO [l, m]
Structure	W	A	A	W or A	A	B	B	N
Lattice Constant	3.186	-	-	3.113		10.813	9.845	4.2112
Atomic Spacing in the (111) plane		-	-	-	-	3.828	3.4807	2.978
Mismatch to GaN (%)	-	-	-	2.3	-	20.1	9.2	-6.5
T _{MP} (K)	2800	1900	2173	3500	2023	2668	2678	3073
Bandgap (eV)	3.4	9	5	6.2	4.7	5.3	6.3	8
Electron Affinity (eV)	3.4	0.9		0 – 2.9		0.63		0.7
Work Function (eV)				0.9 – 1.2		2.1 – 3.3	4	3.1 – 4.4
Dielectric Constant	9.5	3.9	7.5	8.5	14.2	11.4	14	9.8

- a. *Properties of Group III Nitrides*, ed. J. H. Edgar, Inspec, the Institution of Electrical Engineers, London, UK, 1994.
- b. G.W. Kaye, T.H. Laby, *Tables of Physical and Chemical Constants and some Mathematical Functions*, 11th ed, Longmans, New York, 1956
- c. C. T. Sah, *Fundamentals of Solid-State Electronics*, World Scientific, New Jersey, 1991
- d. S.M. Sze, *Physics of Semiconductor Devices*, 2nd edition, Wiley, New York, 1981
- e. "Epitaxially grown AlN and its optical band gap," W.M. Yim, E.J. Stofko, P.J. Zanzucchi, J.I. Pankove, M. Ettenburg, S.L. Gilbert, *J. of Appl. Phys.*, **44**, 292 (1973)
- f. "Electron mobilities in gallium, indium, and aluminum nitrides," W.L. Chin, T.L. Tansley, T. Osotchan, *J. of Appl. Phys.*, **75**, 7365 (1994)
- g. "GaN/AlGaN heterostructure devices: photodetectors and field-effect transistors," M.S. Shur, M.A. Khan, *Mat. Res. Bull.*, **22(2)**, 44 (1997)
- h. S.S. Derbeneva, S.S. Batsano, *Dokl. Chem.*, **175**, 710 (1967)
- i. S.S. Batsonov, E.V. Dulepov, *Soviet Physics – Solid State*, **7(4)**, 995 (1965)
- j. K.A. Gschneider, *Rare Earth Alloys*, Izd. Mir., 1965
- k. "Optical properties and electron energy structure of Y₂O₃ and Sc₂O₃," V. N. Abramov, A. N. Ermoshkin and A. I. Kuznetsov, *Sov. Phys. Sol. State*, **25**, 981 (1983).
- l. "Electronic band structure of magnesium and calcium oxides," N. Daude, C. Jouanin and C. Gout, *Phys. Rev. B*, **15**, 2399 (1977).
- m. G. V. Samsonov, *The Oxide Handbook*, Plenum, New York, 1973, and references therein.

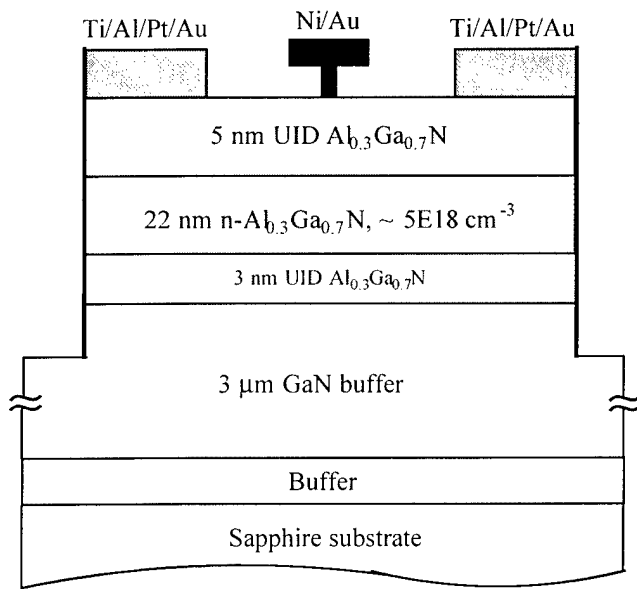
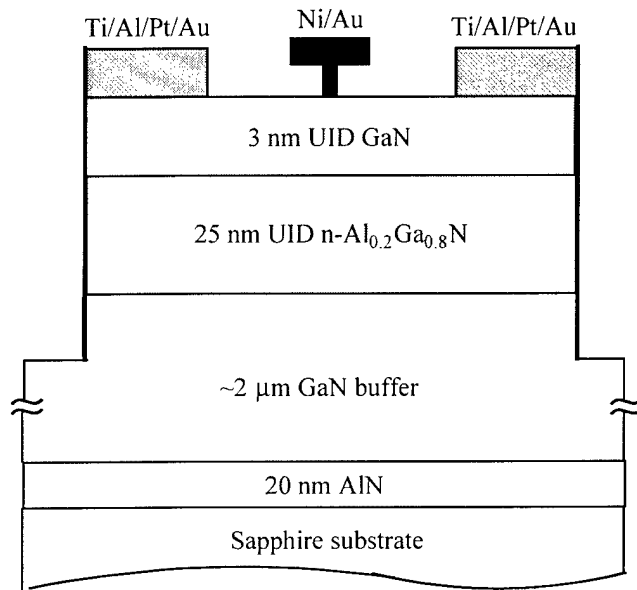


Figure 1. Schematic cross-sections of GaN-cap (top) and AlGaN-cap (bottom) HEMT structures.

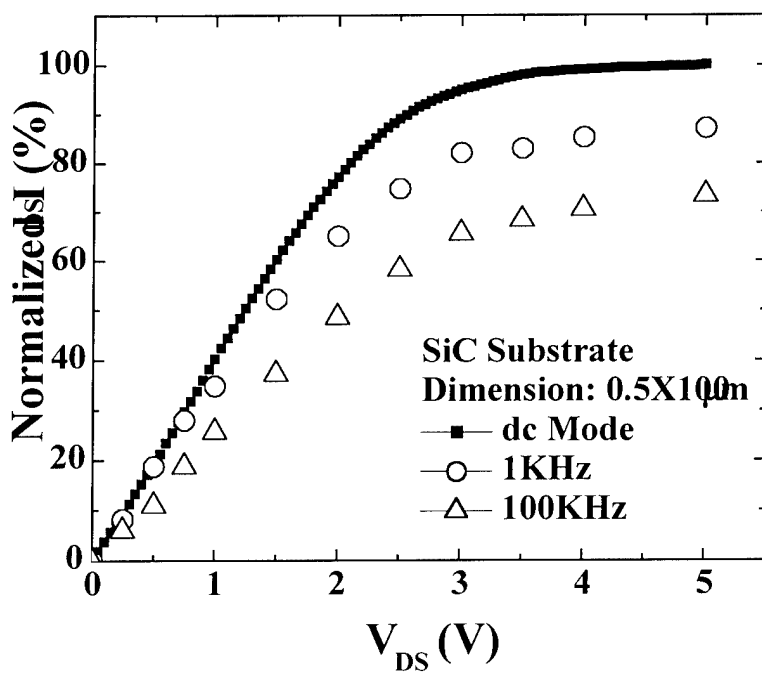
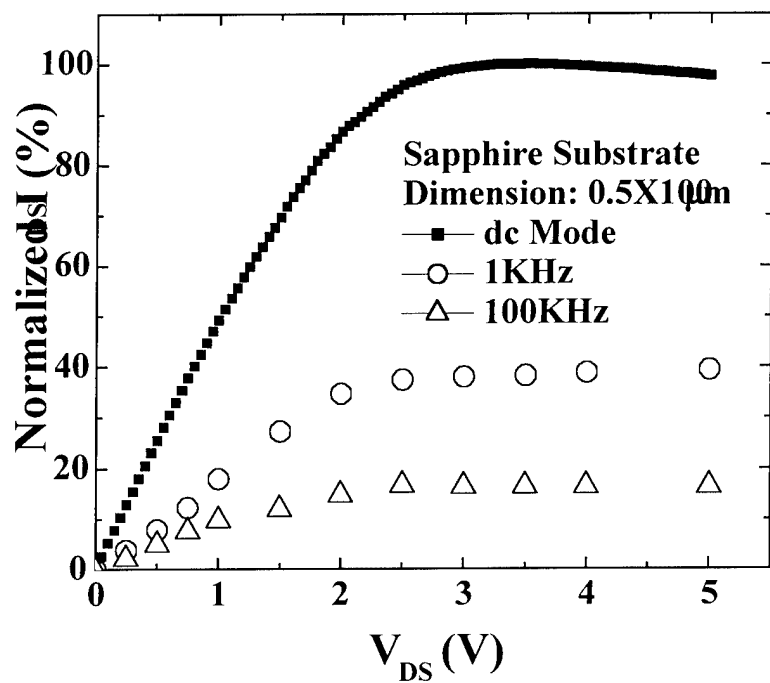


Figure 2. Gate lag measurements on unpassivated 0.5μm gate length, GaN-cap HEMTs grown on either sapphires (top) or SiC (bottom) substrates.

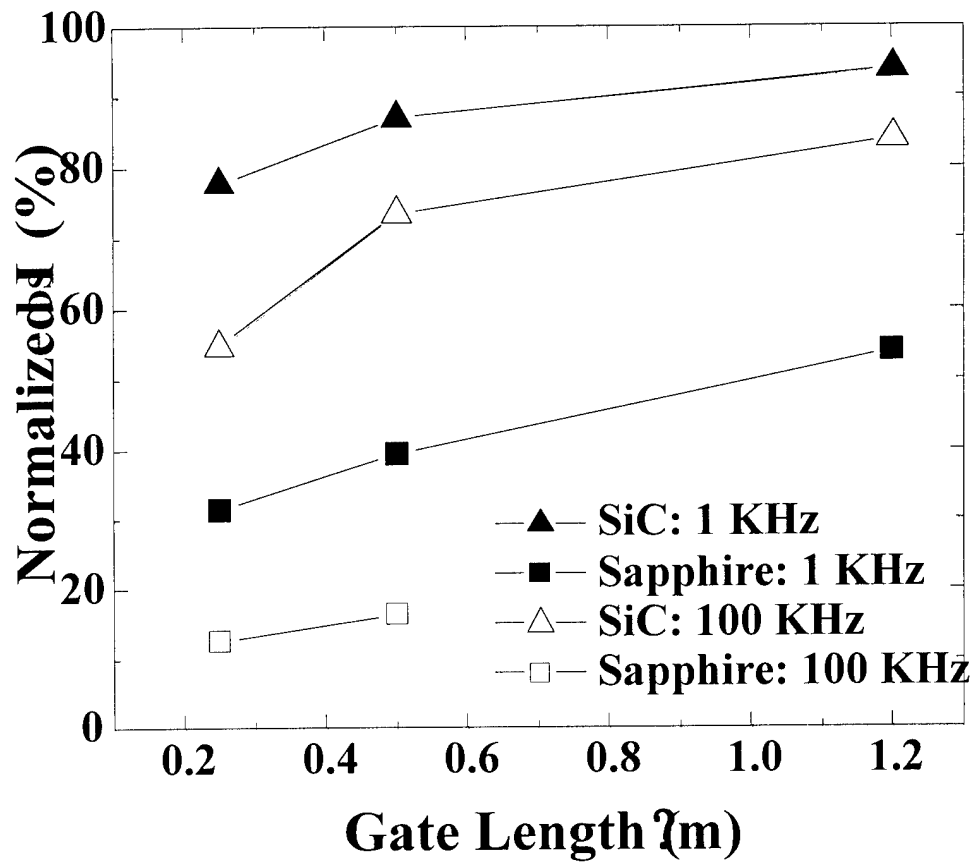


Figure 3. Normalized I_{DS} as a function of both gate length and substrate type for GaN-cap HEMTs at pulse frequency of 1KHz and 100KHz.

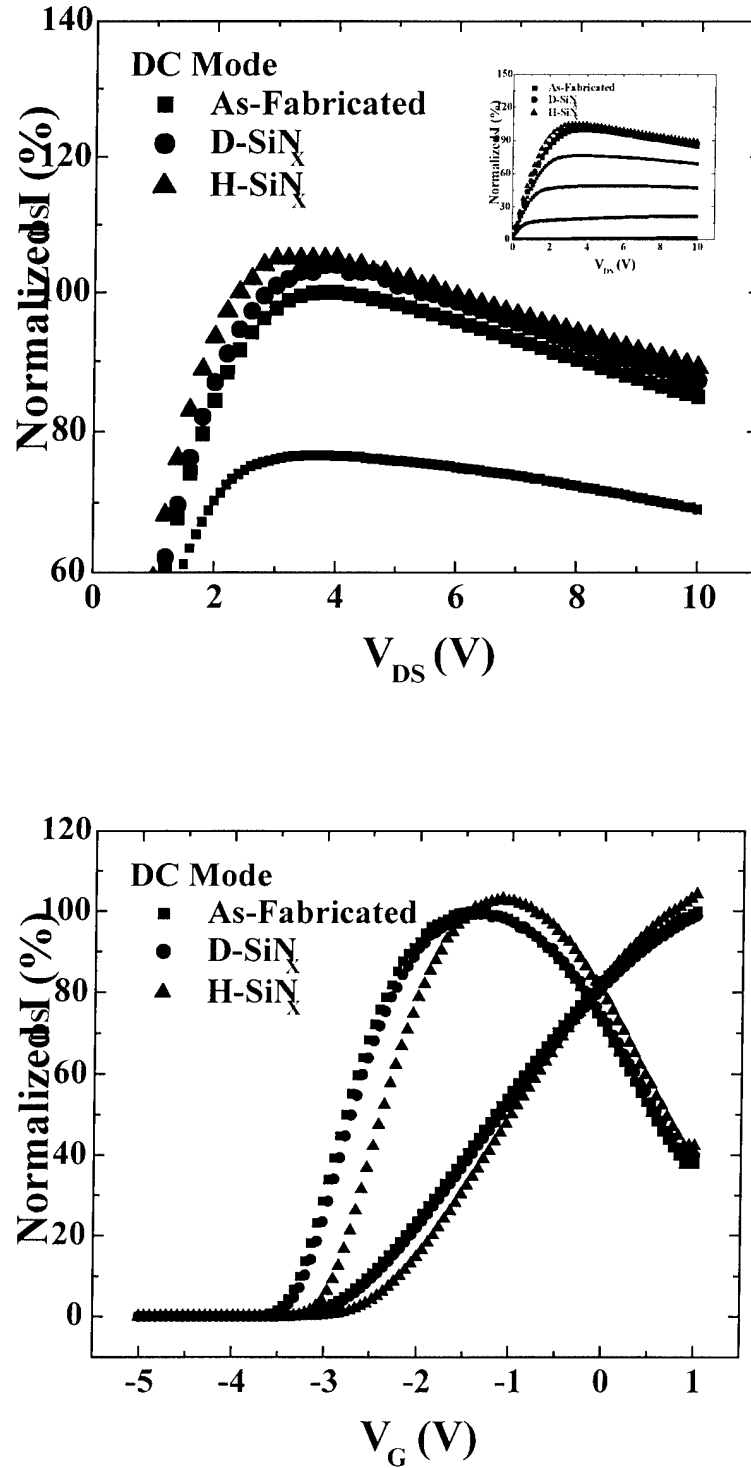


Figure 4. Normalized I_{DS} versus V_{DS} (top) or V_G (bottom) for $1.2 \times 100 \mu\text{m}^2$, GaN-cap HEMTs before and after SiN_x passivation using either hydrogenated or deuterated precursors.

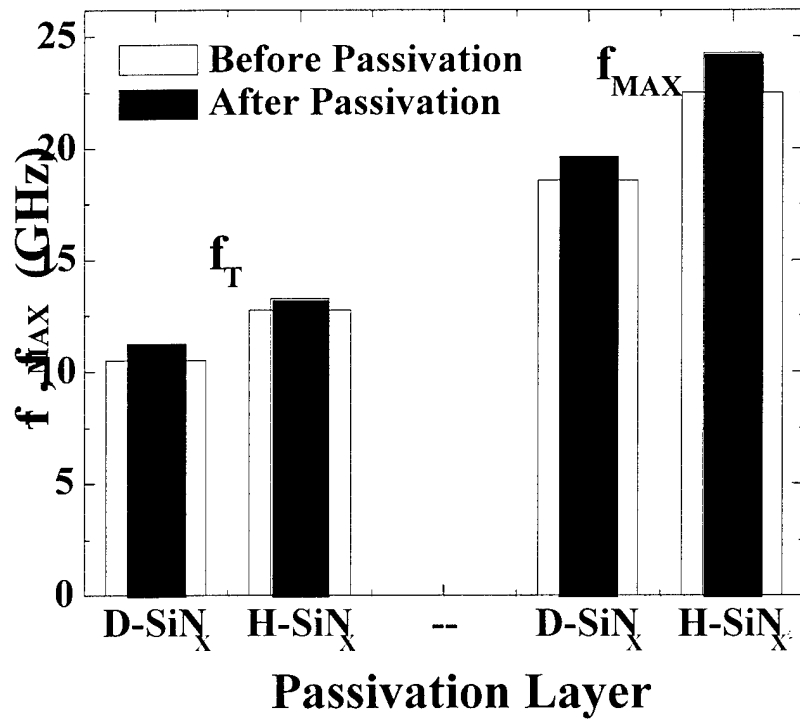
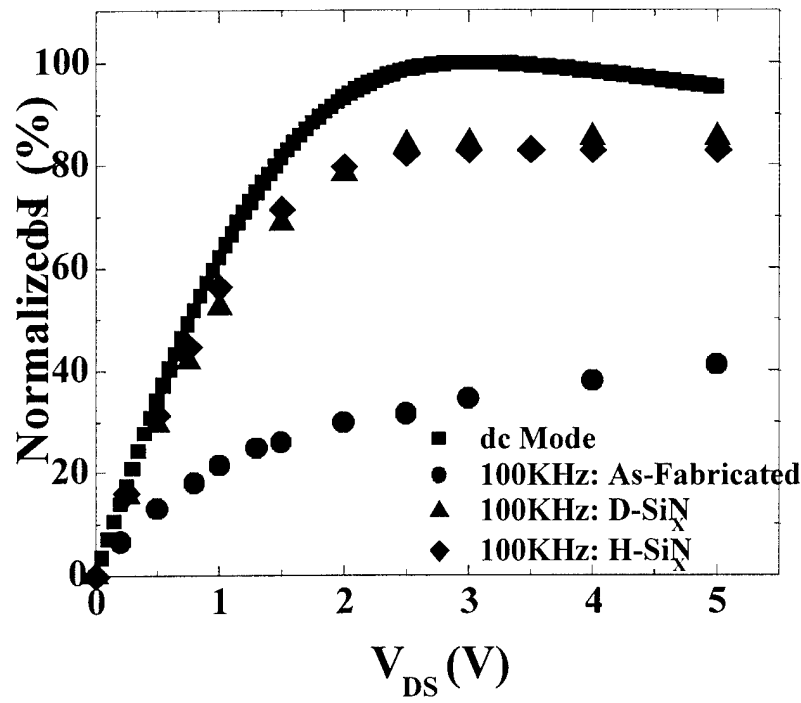


Figure 5. Gate lag measurements before and after SiN_x passivation of $1.2 \times 100 \mu\text{m}^2$, GaN-cap HEMTs (top) and f_T and f_{MAX} before and after SiN_x passivation (bottom).

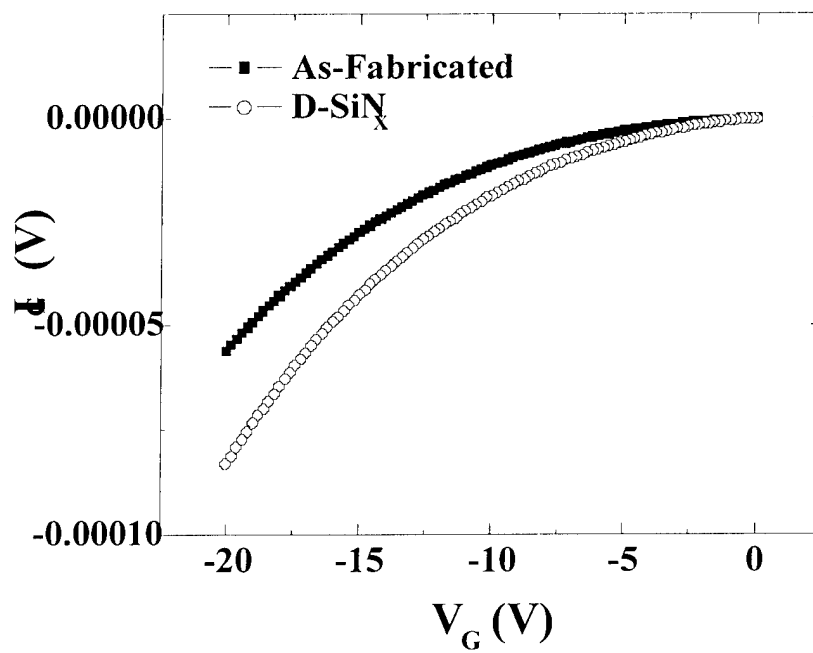
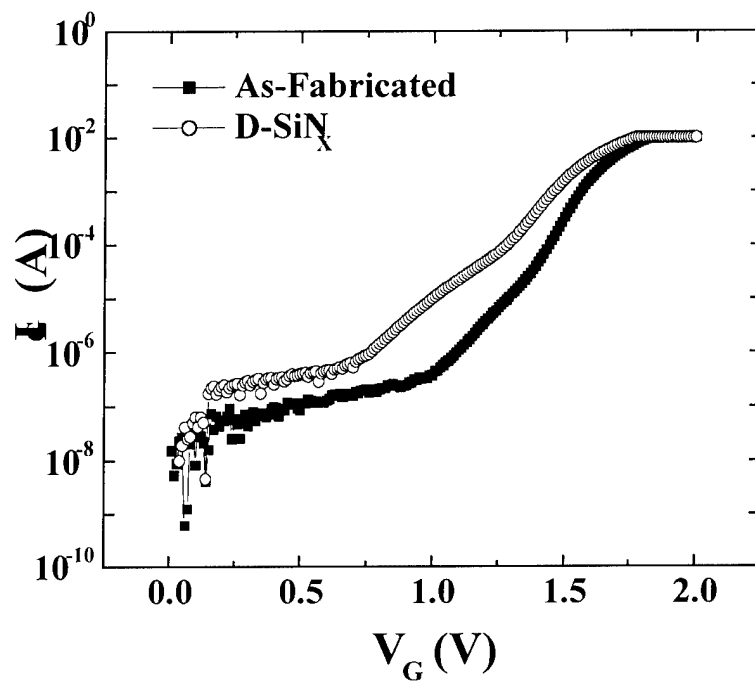


Figure 6. Forward (top) and reverse (bottom) I_G - V_G characteristics from $1.2 \times 100 \mu\text{m}^2$, GaN-cap HEMTs before and after SiN_x passivation with deuterated precursors.

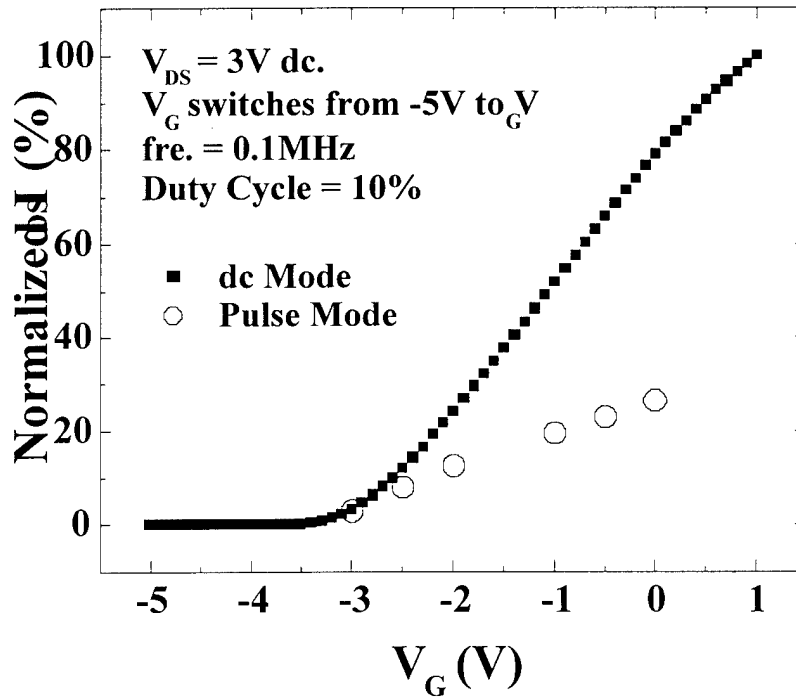
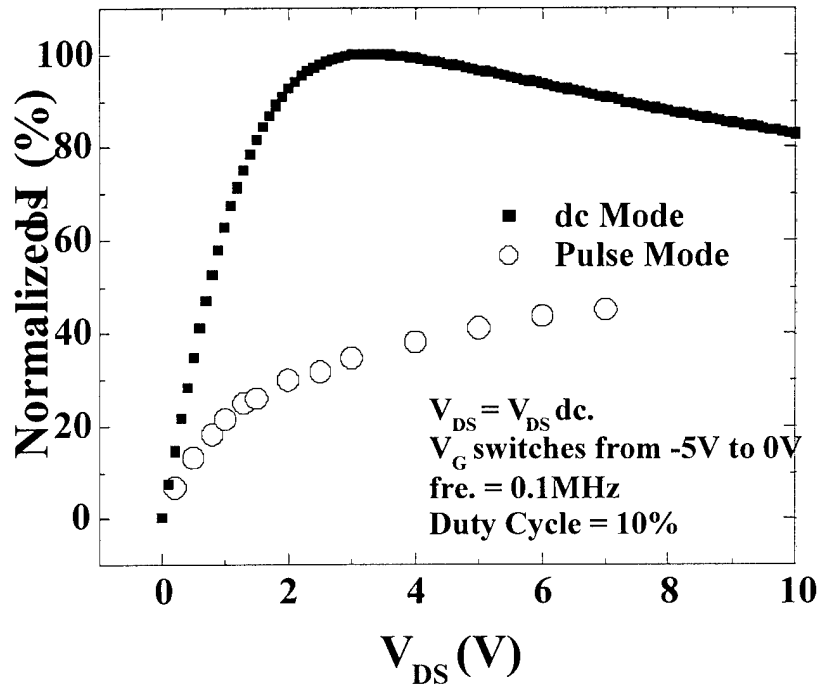


Figure 7. Gate lag measurements on unpassivated GaN-cap HEMTs ($1.2 \times 100 \mu\text{m}^2$ gate). At top V_G was switched from -5 to 0 V, while at bottom it was switched from -5 V to the value shown on the X-axis.

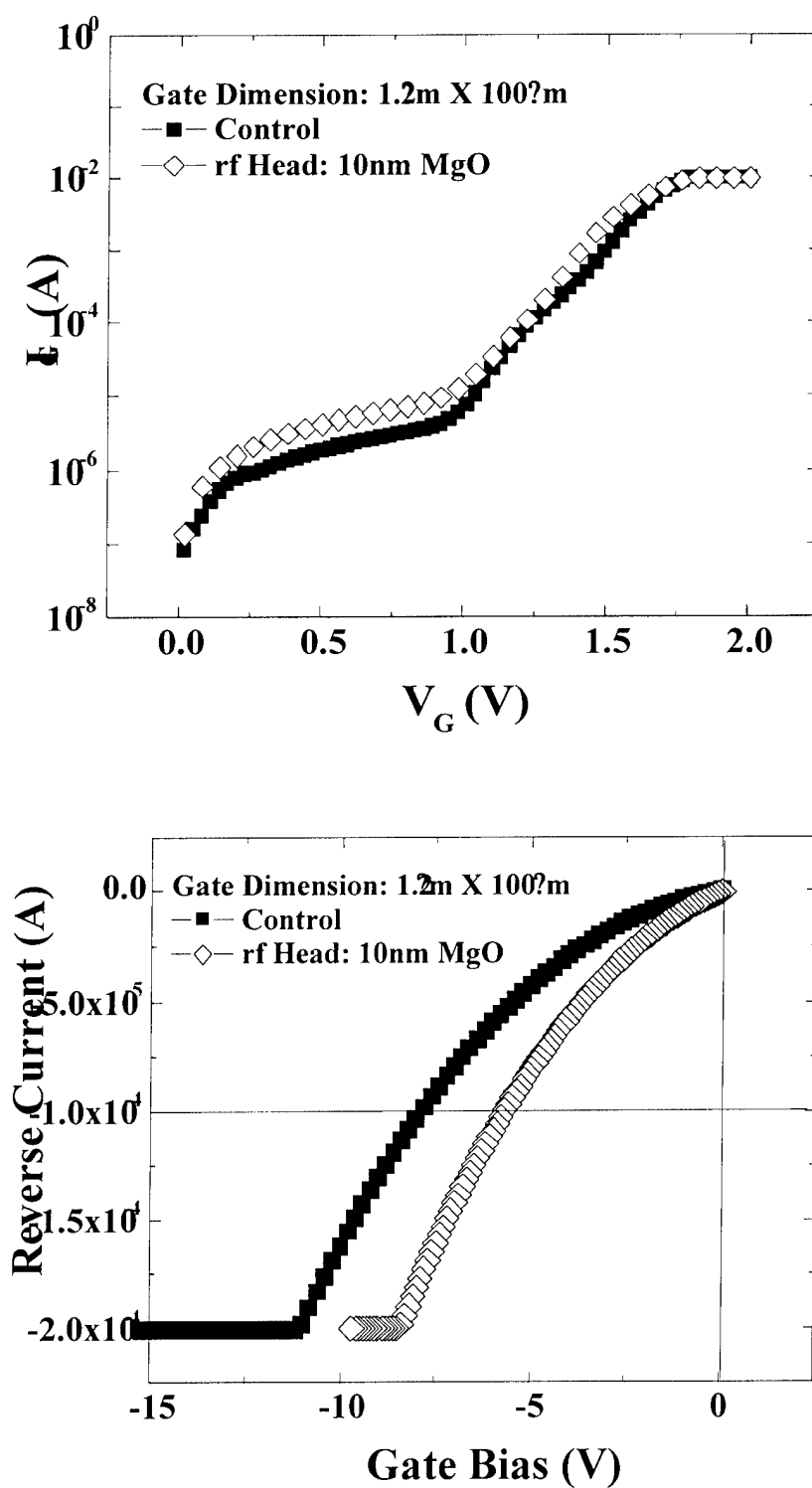


Figure 8. Forward (top) and reverse (bottom) I_G - V_G characteristics from $1.2 \times 100 \mu\text{m}^2$, GaN-cap HEMTs before and after MgO passivation.

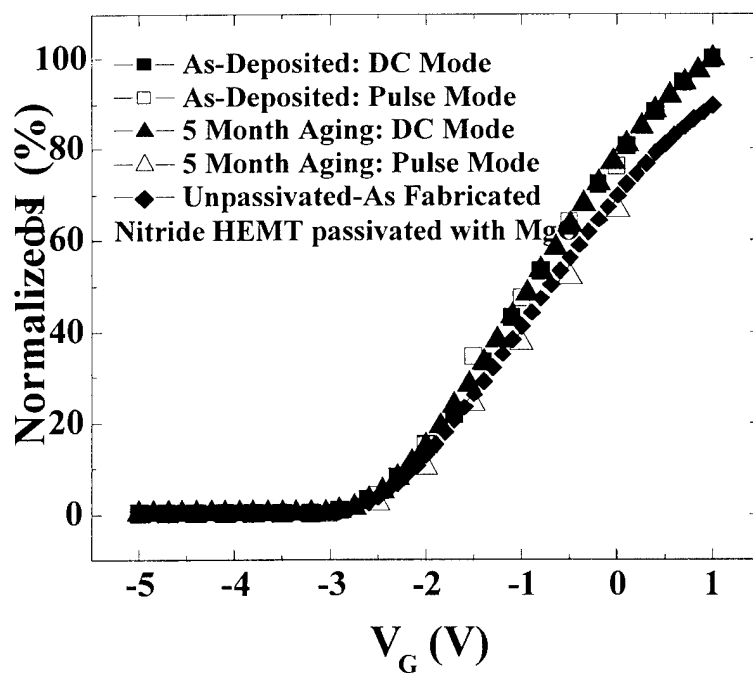
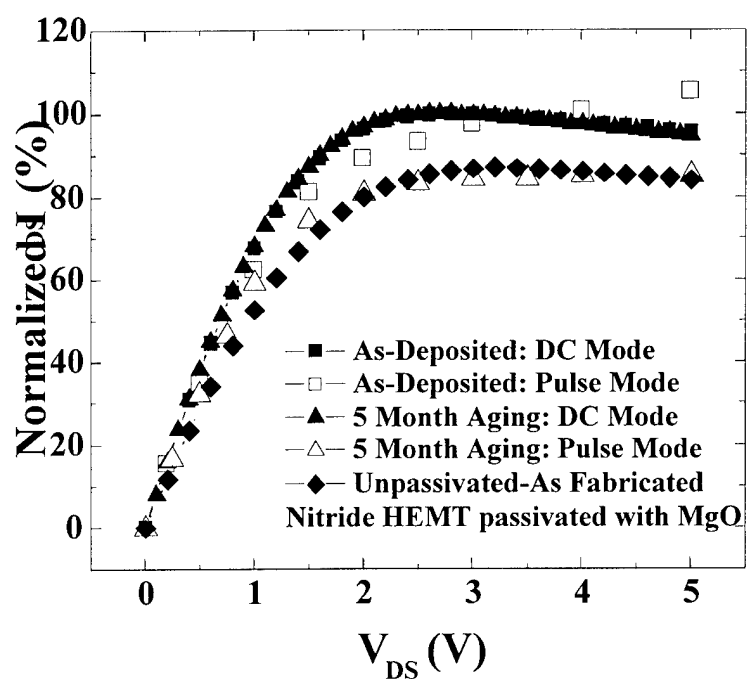


Figure 9. Gate lag measurements before and after MgO passivation and following 5 months aging of $1.2 \times 100 \mu\text{m}^2$, GaN-cap HEMTs. At top V_G was switched from -5 to 0 V, while at bottom it was switched from -5 V to the value shown on the X-axis.

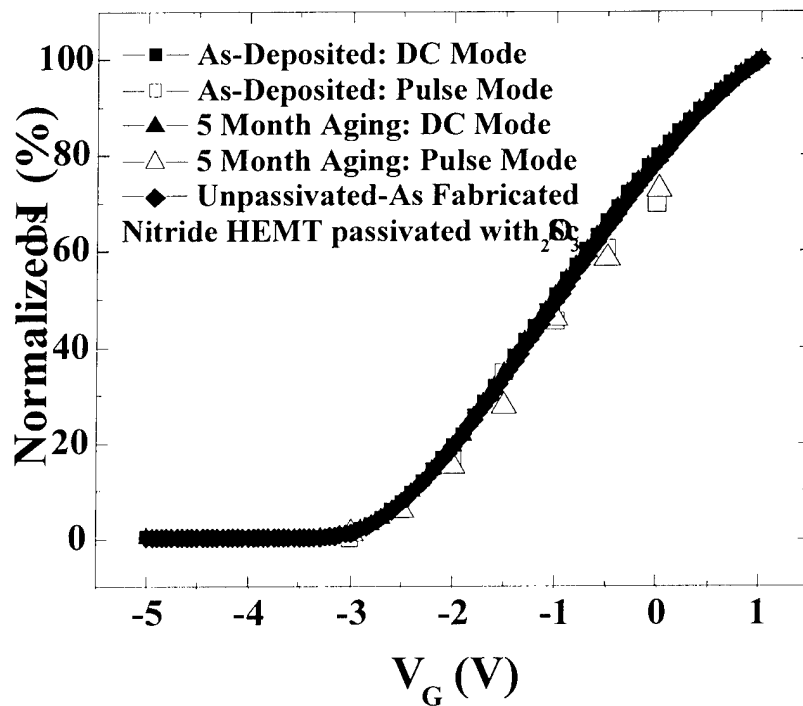
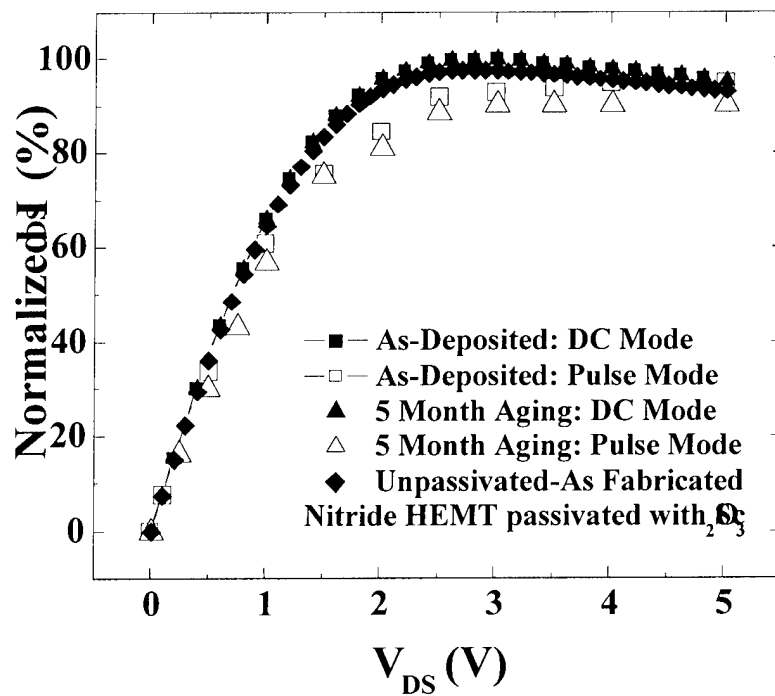


Figure 10. Gate lag measurements before and after Sc_2O_3 passivation and following 5 months aging of $1.2 \times 100 \mu m^2$, GaN-cap HEMTs. At top V_G was switched from -5 to 0V, while at bottom it was switched from -5V to the value shown on the X-axis.

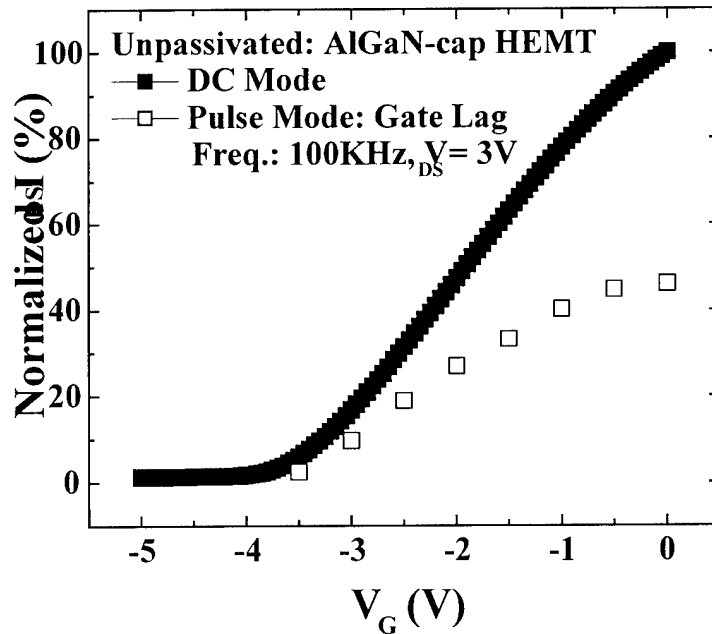
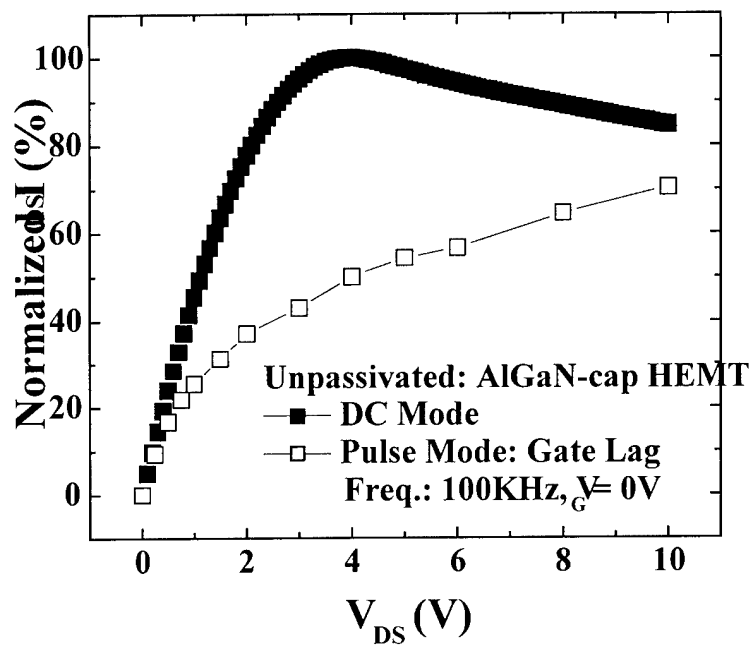


Figure 11. Gate lag measurements on unpassivated 0.5 μ m gate length, AlGaIn-cap HEMTs. At top V_G was switched from -5 to $0V$, while at bottom it was switched from $-5V$ to the value shown on the X-axis.

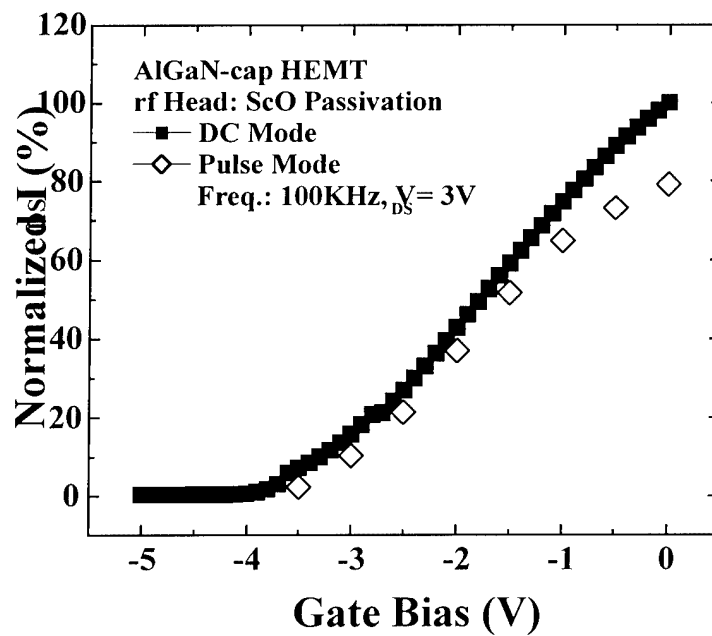
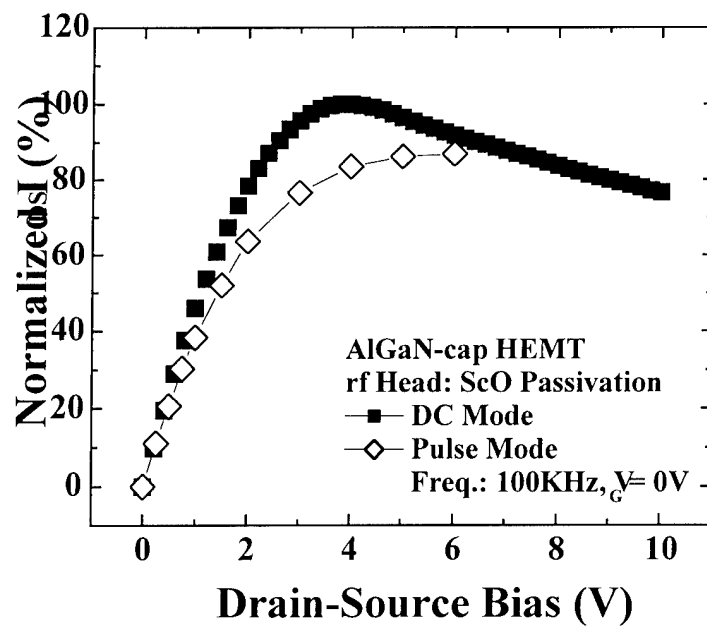


Figure 12. Gate lag measurements before and after Sc_2O_3 passivation of $0.5 \times 100 \mu m^2$, AlGaIn-cap HEMTs. At top V_G was switched from -5 to $0V$, while at bottom it was switched from $-5V$ to the value shown on the X-axis.

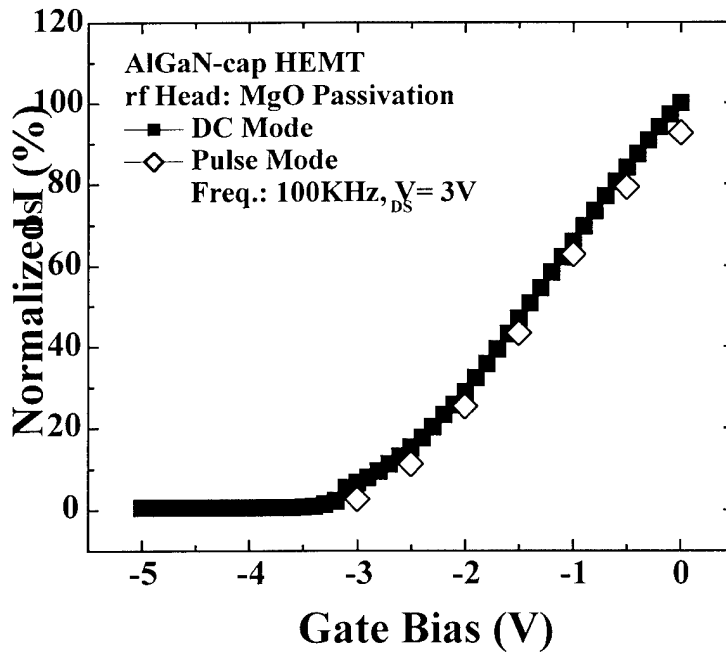
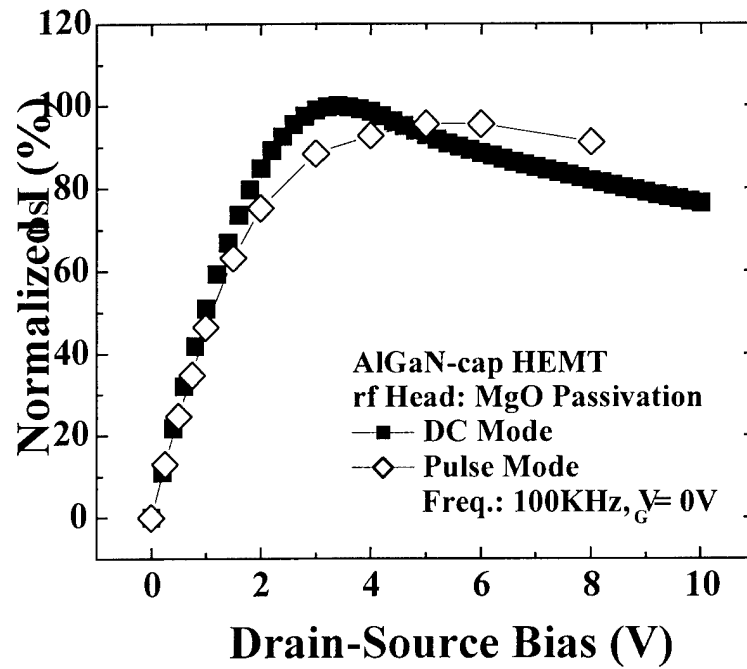


Figure 13. Gate lag measurements before and after Sc_2O_3 passivation of $0.5 \times 100 \mu m^2$, AlGaIn-cap HEMTs. At top V_G was switched from -5 to $0V$, while at bottom it was switched from $-5V$ to the value shown on the X-axis.